Appl. Phys. B 53, 287–295 (1991)

Applied Physics B Photophysics and Laser Chemistry

Second-Order Nonlinear Optical Properties of Poled Coumaromethacrylate Copolymers

M. A. Mortazavi[1,*], A. Knoesen[1,], S. T. Kowel[1,***], R. A. Henry[2], J. M. Hoover[2], and G. A. Lindsay[2]**

[1] Department of Electrical Engineering and Computer Science, University of California, Davis, CA 95616, USA
[2] Polymer Science Branch, Research Department, Code 3858, Naval Weapons Center, China Lake, CA 93555, USA

Received 2 May 1991/Accepted 13 September 1991

Abstract. Second-order nonlinear optical properties of newly designed and synthesized coumaromethacrylate side-chain polymers are reported. The optimum poling conditions were determined experimentally. The optimum poling temperature for these side-chain polymers is well above the glass transition temperature. The second harmonic coefficient of films poled by corona-onset at elevated temperature and the linear electro-optic coefficient of films poled by contact electrodes were measured. The stabilized value of the second harmonic coefficient, d_{33}, at 1064 nm fundamental wavelength was found to be 13 pm/V. The linear electro-optic coefficient, r_{33}, exhibits strong dispersion ranging from 2 to 12 pm/V in the wavelength range 477 to 1115 nm.

PACS: 07.60H, 42.65K, 42.80K, 78.65, 78.20J, 77.40, 81.20S, 81.40R

Polymeric films with large macroscopic second-order nonlinear properties can be created by permanently orienting molecules with large second-order hyperpolarizability within a polymer [1–5]. One method is to deposit a thin film consisting of randomly oriented nonlinear molecules embedded in a polymer host which are then oriented by the application of an external electric field. Even though poled films are not in a state of thermodynamic equilibrium, it has been demonstrated that significant second-order nonlinearities exist for several months after poling [6, 7]. The nonlinear stability can be further enhanced by attaching the nonlinear molecules to a polymer backbone, forming a nonlinear side-chain polymer. In addition to the stability a higher nonlinear chromophore density is possible in side-chain polymers. The higher concentration leads to a larger second-order nonlinear performance, only if the absorption does not significantly increase at the operating wavelengths. Usually a larger second-order hyperpolazibility also implies a chromophore absorbing more strongly at longer wavelengths [8, 9] (600–1000 nm). For such nonlinear polymers increasing the chromophore density is unattractive, since excessive absorption in the near infrared spectrum adversely affects waveguiding devices operating at those wavelengths. An interesting trade-off is to use a side-chain nonlinear polymer that consists of a nonlinear molecular component that has a smaller second-order hyperpolarizability, where the loss in hyperpolarizibility is compensated for by an increase the chromophore concentration. This strategy could potentially result in a higher overall nonlinear performance and a lower absorption at infrared wavelengths. Shifting the absorption spectrum towards shorter wavelengths also permit harmonic generation into the near-UV. Negligible absorption must occur at the fundamental wavelengths, while small absorption can be tolerated at the second-harmonic wavelength.

In this paper we report the results of an electro-optical investigation of one such a nonlinear side-chain polymer, poly(methyl methacrylate-co-coumaro methacrylate) (P(MMA-CMA)). Various molecular weights and mole percent CMA polymers were investigated (see Table 1). Two poling techniques have been used to produce optical nonlinear films. Contact electrode poling is particularly simple to implement and the resulting stratified film structure maybe suitable for electro-optic modulator applications. Corona-onset poling at elevated temperature (COPET) [6, 7] is particularly effective in achieving large orientational order and the resulting films are suitable for second harmonic generation applications. Hayden et al. [10] characterized one low molecular weight COPET

* New address: Hoechst Celanese, 86 Morris Avenue, Summit, NJ 07901-3956, USA
** Person to whom all correspondence should be addressed
*** New address: Department of Electrical and Computer Engineering, University of Alabama in Huntsville, Huntsville, AL 35899, USA

Table 1. The chromophore density (molecules/cm^3), glass transition temperature (°C), number average molecular weight, weight average molecular weights and mole percent CMA of P(MMA-CMA) side-chain polymers used

Sample lab book #	Doping density	T_g [°C]	$\langle M_n \rangle$ [Daltons]	$\langle M_w \rangle$ [Daltons]	Mole % CMA
P(MMA-CMA)-2 1220-35	2.2×10^{20}	109	23000	38000	3.4
P(MMA-CMA)-3 1220-34	3.3×10^{20}	111	20000	30000	5.5
P(MMA-CMA)-6 1220-48	5.7×10^{20}	93	18000	≈ 60000	10.5
P(MMA-CMA)-9 1253-6	9.0×10^{20}	111	≈15000	≈ 58000	21
P(MMA-CMA)-10 1220-30	9.8×10^{20}	116	14000	20000	23
P(MMA-CMA)-11 1295-6	9.8×10^{20}	135	49300	101000	23

P(MMA-CMA) side-chain polymer (i.e. P(MMA-CMA)-9 in Table 1). The second harmonic coefficients were determined by polarization sensitive second harmonic measurements ($d_{33} = 11$ pm/V at 1064 nm, fundamental). The linear electro-optic coefficient was determined by waveguiding techniques ($r_{33} = 3.5$ pm/V at 780 nm). In this paper a range of higher molecular weight (MMA-CMA) polymers are investigated and poled by contact electrodes and COPET. For COPET films the dependence of the orientational order on the poling temperature and poling current was determined. The relaxation of the nonlinearities of a poled film when exposed to a temperature well exceeding room temperature was investigated. The second-order nonlinearities were characterized by second harmonic and linear electro-optic measurements. The electro-optic coefficients were determined by electro-optic reflection polarimetry. The dispersion of the linear electro-optic coefficient was measured and compared to theory. Our group has recently reported the harmonic generation of 315 nm, 14 fs pulses utilizing COPET P(MMA-CMA) polymer films [11].

1 Experiment

1.1 Synthesis and Characterization of P(MMA-CMA)

The P(MMA-CMA) nonlinear polymer (NLP) consists of a nonlinear optical donor-acceptor, coumarin side-chain chromophore *N*-(3-methacryloxyalkyl)-7-diethylaminocoumarin-3-carboxamide (CMA) (see Fig. 1) attached to a methyl methacrylate (MMA) backbone [12, 13] (see Table 1). Various chromophore densities were synthesized. P(MMA-CMA) was prepared by a free radical initiated solution-polymerization of methyl methacrylate and coumaro methacrylate in tetrahydrofuran [12] (THF). The copolymer was purified by preparative gel permeation chromatography (GPC) with Styragel® columns, using chloroform and a flow rate of 15 ml/min. The average molecular weights were determined by GPC based on polystyrene standards using THF. The glass transition temperatures were measured with a differential scanning calorimeter (DuPont 1090) using a heating rate of 10° C/min. The mole percent CMA was determined by 80 MHz proton nuclear magnetic resonance. The complex

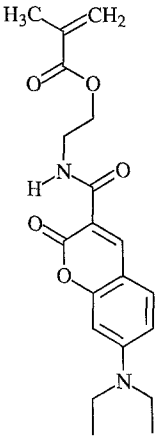

Fig. 1. Chemical structure of N-(3-methacryloxyalkyl)-7-diethylaminocoumarin-3-carboxamide monomer

dielectric permittivity was measured versus temperature at 0.1 Hz (DuPont DEA 4.2 A).

1.2 Film Preparation

Films were made on BK7, quartz, pyrex, or indium tin oxide (ITO) covered substrates depending on the requirements of the intended characterization technique. In the 0.5–2.0 μm thickness range, spin-cast films were prepared by controlling the viscosity and the spinning speed which ranged between 1000 and 2000 rpm. In the 2.0–5.0 μm thickness range, blade-cast films were prepared by controlling the viscosity and blade-to-substrate gap. Residual solvent was removed by heat treating the films at 150° C, 0.5 mm Hg vacuum for 12 h. Special attention to solvent removal and subsequent thermal annealing is essential since residual solvent and microvoids are known to lower the glass transition temperatures [14] and effect the orientational relaxation [15] behavior of the polymers.

Films were poled by the COPET technique using a parallel wire electrode configuration [7]. The polymeric films were deposited onto a substrate such as BK7 or Pyrex microscope slides and placed on top of a grounded metallic planar electrode. These substrates have sufficient conductivity to pass the poling currents to the planar electrode. The poling configuration consisted of a 40 μm diameter tungsten wire, 2 cm long, suspended 1 cm above

the polymeric film to which a variable voltage up to 10 kV can be applied. A 10 MΩ resistor connected between voltage supply and electrode served as a current limiter. Another 10 MΩ resistor connected between the planar electrode and ground served as a current sensing element. This poling configuration produced a poled strip on the substrate that is approximately 1 cm wide by 2 cm long (this corresponds to the length of the wire). The length of the wire and placement of the slide should be such that no significant poling current can pass around the substrate and flow directly to the grounded electrode. The grounded electrode should extend the poling area to prevent high current density regions in the polymeric film. While the film was at a fixed elevated temperature, the poling current was controlled by adjusting the voltage applied to the wire electrode. After approximately five minutes, while holding the voltage constant, the temperature of the film was gradually lowered to room temperature. Second harmonic measurements were made on corona poled films. Linear electro-optic measurements were made on contact electrode poled films. A 5 μm thick polymer film was blade-cast deposited onto a 25 nm thick ITO layer covering a glass substrate. A 100 nm thick gold layer was vacuum deposited onto the polymer film. The film was poled with a 1 MV/cm electric field at 150° C for 5 min and cooled down to room temperature with the electric field maintained.

1.3 Optical Characterization

1.3.1 Linear Properties. Absorption spectroscopy of films was performed with a UV–VIS spectrophotometer (Perkin Elmer Lambda-4). Film thickness and refractive index measurements were made by a guided mode attenuated total reflection technique [16]. The in-coupling angles of TE or TM guided modes were measured with a prism coupling instrument (Metricon PC-2000) modified for multi-wavelength measurements. Refractive index dispersion measurements were made at the following discrete laser wavelengths; Ar: 477, 488, 502, 514 nm, He–Ne: 632 nm, and Nd:YAG: 1064 nm. The film thickness obtained at different wavelengths correlated within 5%. Final verification of the film thickness was obtained with a stylus profilometer (Dektak 3030).

1.3.2 Nonlinear Properties. Second harmonic generation was used to measure the nonlinear susceptibility, to probe long-term orientational stability, and to study thermally stimulated orientational relaxation of nonlinear properties. A Nd:YAG laser (Spectra-Physics GCR-11) was used to perform second harmonic measurements ($\lambda = 1064$ nm, Q-switched at 10 Hz, 100–200 mJ per 10 ns and 0.2 cm^2 unfocused beam). A photomultiplier detector and boxcar averager (Stanford Research SR280) was used to average over 10 pulses. The second harmonic intensity of the films was measured with parallel polarized (p) excitation and p-detection. The second harmonic intensity was compared to the second harmonic generated by a quartz reference, $d_{11} = 0.45$ pm/V.

A hot stage was designed for the thermally stimulated orientational relaxation studies to provide accurate temperature control while the second harmonic signal was monitored, see Fig. 2. A temperature controller (Omega CN-9000) controlled the power to electrical heating tapes wrapped around an aluminum stage. The temperature of the sample was monitored with thermocouple placed on the film. The temperature was controlled within ±2° C. The following precautions were taken to ensure that optical stability and electronic stability were maintained over experimental time periods lasting up to 40 h. For optical stability, the second harmonic signals from a quartz reference channel and the sample channel were collected separately by two boxcars averagers. The two output pulse trains were digitized by two analogue to digital converters and accumulated by two digital buffers (Stanford Research SR245). The two signal channels were thus collected in real time, and at regular intervals transferred by a general purpose interface bus to a magnetic storage disk. The experiment was controlled by a computer (MAC II with National Instruments Labview software). Electronic post-processing compensated for laser power fluctuations. For electronic stability, the boxcar averagers

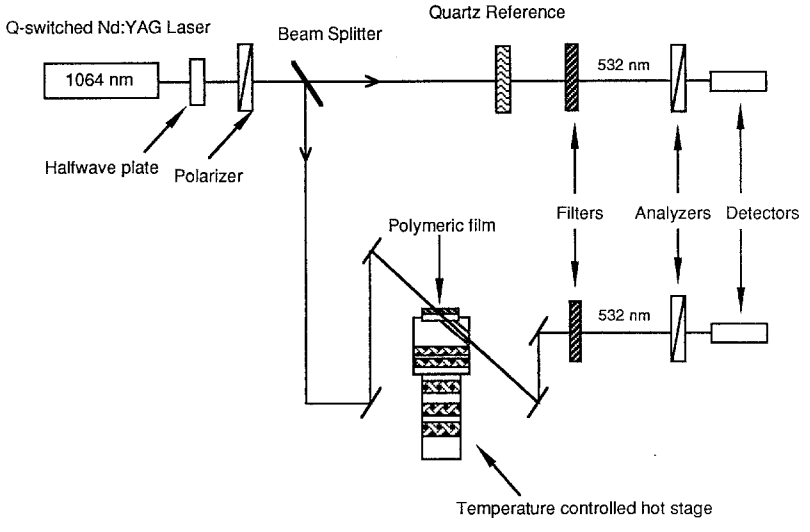

Fig. 2. Experimental configuration used to study the elevated temperature relaxation behavior of poled P(MMA-CMA) polymeric films

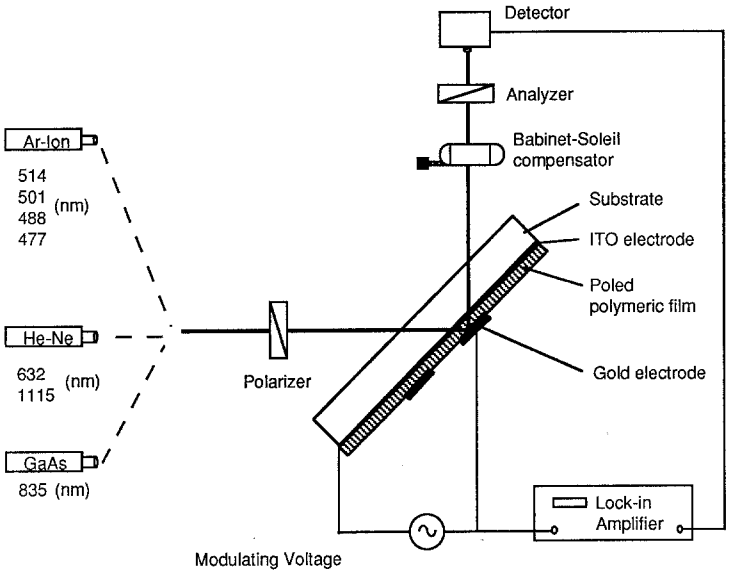

Fig. 3. Experimental configuration used for the electro-optic coefficient measurement

were configured in an active baseline subtraction mode to significantly reduce electronic long term dc baseline drifts [17] in the electronic circuitry.

A reflection modulated technique [18, 19], see Fig. 3, was used to determine the dispersion of the linear electro-optic coefficient. The NLP index of refraction was modulated by a voltage applied to two parallel electrodes. One electrode was a transparent ITO layer and the other was a reflecting Au layer. An input beam polarized at 45° to the plane of incidence was reflected off the Au layer and passed through an analyzer. A Soleil-Babinet compensator was adjusted to bias the optical system in a linear modulation regime which occured at half the maximum output intensity as measured by a photo detector. A sinusoidal modulating voltage (20 V rms 1 kHz) was applied across the polymeric film with ITO and Au layers serving as conducting electrodes. The modulation of the output intensity was synchronously detected by a lock-in amplifier (Stanford Research SR530). The spurious modulation resulting from the first reflection off the glass film interface was minimized by subtracting the total modulation signal at two alternate optical bias positions (see [19]). Electro-optic properties were measured at the following discrete laser wavelengths; Ar: 477, 488, 502, 514 nm, He–Ne: 632, 1115 nm, and GaAs: 835 nm.

2 Results and Discussions

2.1 Linear Optical Properties

The absorption spectrum of a P(MMA-CMA) side-chain polymer film is shown in Fig. 4. A large second-order hyperpolarizability in a chromophore is often achieved by increasing the length of a π-conjugate link between the donor and acceptor groups, usually with the result of a strongly red shifted absorption spectrum. A film system absorbing at these longer wavelengths could be undesirable for guided wave optical applications. In poled film systems one compromise consists of using a chromophore with a lower hyperpolarizability with attendant low absorption at the longer wavelengths [8, 9]. Table 2 compares the λ_{max}, full width half maximum (FWHM), dipole moment (μ), and molecular hyperpolarizability (β), of a mixture of PMMA and 4-(N-ethyl-N-(2-hydroxyethyl))amino-4′-nitroazobenzene (Disperse Red 1

Table 2. Comparison of the absorption spectra of PMMA/DR1 mixture and P(MMA-CMA) side-chain polymers

Material	λ_{max} [nm]	FWHM [nm]	μ [D]	β 10^{-30} [cm^5/esu]
PMMA/DR1	490	121	8.7	47
P(MMA-CMA)-3	410	69	5.02	20.7

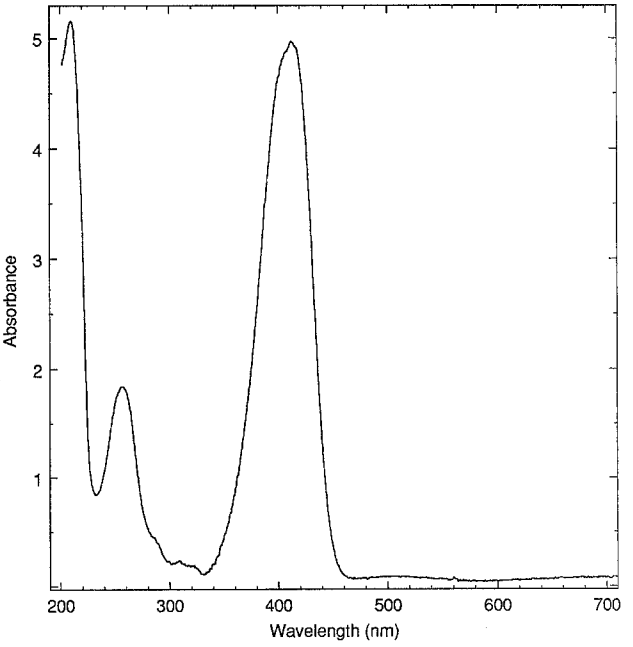

Fig. 4. Absorption spectrum of P(MMA-CMA)-11 film scaled to 1 μm film thickness

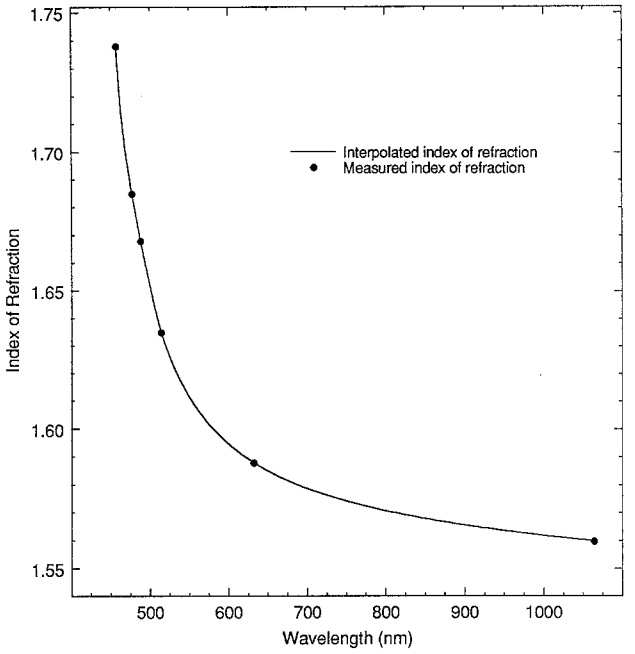

Fig. 5. Index of refraction of P(MMA-CMA)-11 film as a function of wavelength

or DR1) (PMMA/DR1) [7] and P(MMA-CMA). Semi-empirical molecular orbital calculations (YMP Cray, MOPAC 5.0) were used to obtain μ and β. PMMA/DR1 has a larger β, absorbs at longer wavelengths and is representative of a large class of nonlinear polymers. P(MMA-CMA) has a smaller β, but absorbs at shorter wavelengths.

The nonlinear coefficient calculations from experimental measurements invariably requires the knowledge of the index of refraction n at multiple wavelengths. The value of n strongly influences the accuracy of the nonlinear constant measurements (see (1) and (6)). The result of an index of refraction dispersion measurement on an unpoled P(MMA-CMA) film is shown in Fig. 5. The birefringence induced by poling and induced piezo-electric effects have not been taken into account in this study.

2.2 Nonlinear Optical Properties

2.2.1 Second Harmonic Generation. Accurate second harmonic coefficient measurements based on Maker fringes [20] are possible if the nonlinear material is several coherence lengths thick. The coherence length in a nonlinear film is given by $L_c = 0.25\lambda^{\omega}/(n^{2\omega}\cos\theta^{2\omega} - n^{\omega}\cos\theta^{\omega})$, where n is the index of refraction, θ is the angle of propagation inside the film, the superscripts ω and 2ω refer to the fundamental and second harmonic wavelengths. In a Maker fringe thin film experiment, the second harmonic intensity is recorded as a function of optical pathlengths by varying the angle of incidence. The Maker fringes are the result of constructive and destructive interference between the fundamental and second harmonic fields. Maker fringes are absent if the film thickness is less than the coherence length. Typically the coherence length of nonlinear polymeric films is greater than the polymeric film thickness. For example, from index dispersion measurements, the coherence length of P(MMA-CMA) at 1064 nm fundamental wavelength was estimated at 3.4 μm at normal incidence and the polymer film thickness was typically 1 μm. A reasonable estimate of d_{eff} can be obtained by performing measurements with p-excitation, p-detection, and at the Brewster angle [7]. The measurement of the second harmonic intensity produced by the film ($I_{\text{fb}}^{2\omega}$) was made relative to second harmonic intensity produced by a quartz reference ($I_{\text{q}}^{2\omega}$), and the effective d-coefficient

$$d_{\text{eff}} = \frac{2d_{\text{q}}L_{\text{qc}}T_{\text{q}}^{1/2}(\varepsilon_{\text{f}}^{\omega}\sqrt{\varepsilon_{\text{f}}^{2\omega}})^{3/2}\cos\theta_{\text{f}}}{\pi L_{\text{f}}(\varepsilon_{\text{q}}^{\omega}\sqrt{\varepsilon_{\text{q}}^{2\omega}})^{3/2}\,\text{sinc}\left[\dfrac{\pi L_{\text{f}}}{2L_{\text{qf}}}\right]}\sqrt{\frac{I_{\text{fb}}^{2\omega}}{I_{\text{q}}^{2\omega}}}, \tag{1}$$

where L_{f} is the film thickness, T is the product of the electromagnetic power transmission factors of the fundamental and second harmonic waves, ε is the permittivity, L_{qc} and L_{qf} are the coherence length of the quartz reference and the film respectively, θ_{f} is the angle between the boundary normal and the direction of phase propagation inside the film, $\text{sinc}(x) = \sin(x)/x$, and $d_{\text{q}} = 0.46\,\text{pm/V}$. Multiple boundary reflection, and absorption at second harmonic and fundamental wavelengths were neglected.

The largest second harmonic coefficient, d_{33}, is related to the effective nonlinear coefficient, d_{eff}, through the projection factor

$$d_{33} = \frac{d_{\text{eff}}}{\left[\dfrac{2}{\Lambda}\cos\theta_{\omega}\sin\theta_{\omega}\cos\theta_{2\omega} + \left(\dfrac{1}{\lambda}\cos\theta_{\omega}^2 + \sin\theta_{\omega}^2\right)\sin\theta_{2\omega}\right]}, \tag{2}$$

where $\Lambda = d_{33}/d_{13}$. In the low poling field limit $\Lambda = 3$, a value often achieved with contact-electrode poling. In the case of COPET films Λ was between 3 and 4, indicative of the high electric field during poling. This large Λ has been reported by several investigators [7, 10, 21]. Thus, it is important not to assume the low poling field limit for COPET films when d-coefficient calculations are made.

The parameter Λ of corona poled films was calculated from the order parameter

$$\Phi = \frac{1}{2}\left[(3\langle(\cos\theta)^2\rangle - 1)\right]. \tag{3}$$

It was shown previously that for COPET films Φ can be determined from spectroscopic absorption data of the films before and after poling [7, 21]. This measurement technique was used to determine Φ for the COPET films. The statistical moments are given by $\langle(\cos\theta)^n\rangle = L_n(-\Gamma)$, where $L_n(-\Gamma)$ is the n^{th} order Langevin function and Γ is the ratio of electrostatic dipole alignment energy to thermal energy. Under the assumption of the rigid oriented gas model (ROGM) [7], d_{33} should be proportional to the statistical moment $\langle\cos^3\theta\rangle$ and d_{13} should be propor-

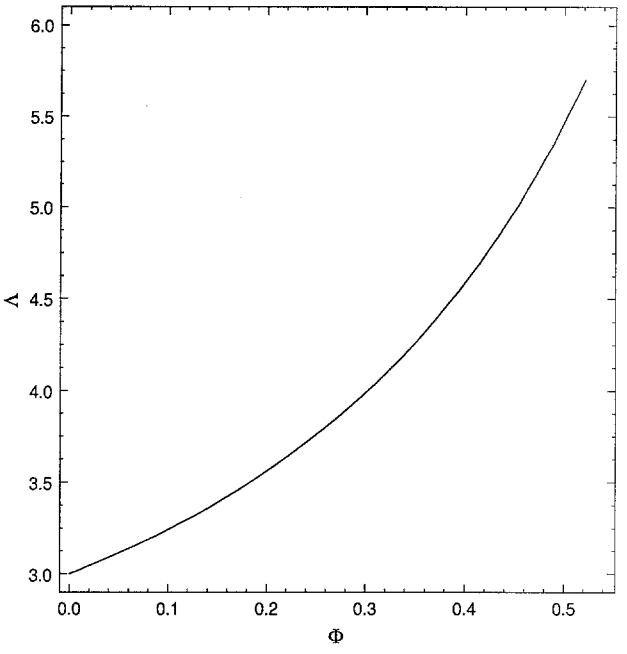

Fig. 6. Theoretical plot of the ratio $d_{33}/d_{13} = \Lambda$ vs the order parameter Φ

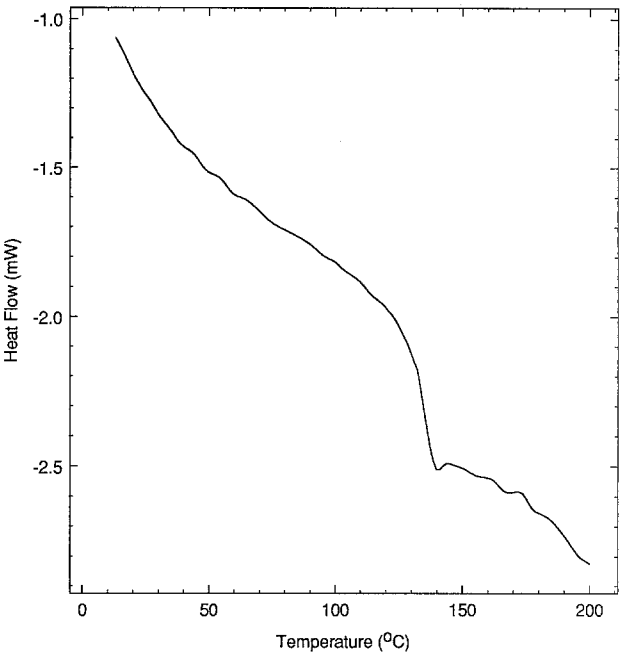

Fig. 7. Differential scanning calorimetry scan of P(MMA-CMA)-11

tional to $\langle \cos\theta \sin^2\theta \rangle$. The parameter Λ can be expressed in terms of Γ and Φ as

$$\Lambda = \frac{d_{33}}{d_{13}} = (1 - \Phi)\frac{\Gamma^2}{3\Phi} - 2 \tag{4}$$

and parameters Φ and Γ have the following inter-dependance:

$$\Phi = 1 + \frac{3}{2}\left(\frac{2}{\Gamma^2} - \frac{2}{\Gamma}\coth\Gamma\right). \tag{5}$$

Figure 6 shows a plot of Λ as a function of Φ. Another method of determining Λ is by second harmonic generation measurements utilizing multiple polarizations for excitation and detection [10].

The optimal COPET conditions for the P(MMA-CMA) films were determined experimentally by varying the corona current and the poling temperature. It was found that by increasing in the poling current past 2 μA provided no further enhancement in the observed second harmonic intensity measured several days after poling. This observation was consistent with independent in-situ second harmonic experiments to optimize corona poling voltage [22]. These experiments also showed a saturation of the second harmonic signal as the poling voltage was increased. In our studies by keeping the poling current at or above 2 μA, the orientational order was repeatable at each temperature, but a strong dependence on the poling temperature was observed. This behavior was investigated in an experiment that kept the corona current fixed at 2 μA, while the poling temperature was increased from below the glass transition temperature to ≈ 60° C above T_g. The DSC scan of P(MMA-CMA)-11 is shown in Fig. 7. The same sample was repeatedly poled at higher temperatures. Between each poling run, sufficient time elapsed to discount enhancement of second harmonic properties by residual charge. Before poling the sample again at a higher temperature, the film was thermally annealed at approximately 160° C for at least 5 h. Figure 8 shows the stabilized values of the second harmonic $d_{\text{eff}}/d_{\text{quartz}}$ versus the poling temperatures while keeping the corona current constant. Other films poled only at 160° C and 2 μA exhibited similar $d_{\text{eff}}/d_{\text{quartz}}$ values. It was thus concluded that the poling and thermal history of the sample that was used to obtain the results

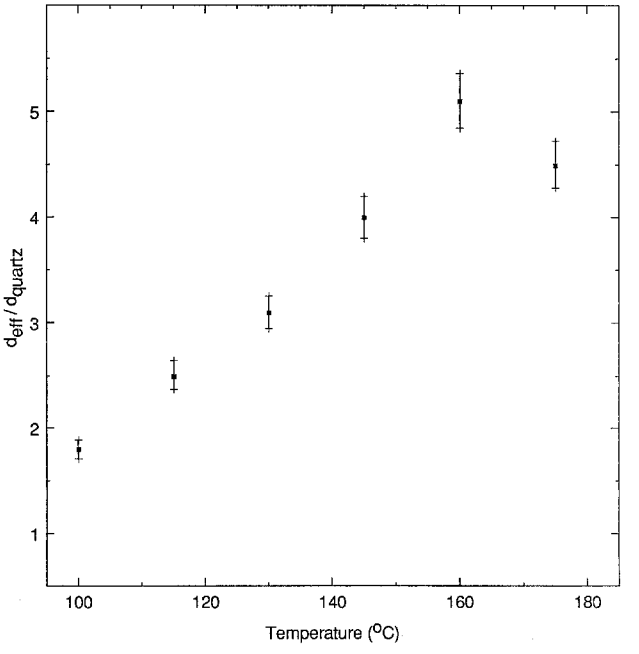

Fig. 8. The second harmonic $d_{\text{eff}}/d_{\text{quartz}}$ for COPET P(MMA-CMA)-3 side-chain polymer film as a function of poling temperature with poling current held fixed at 2 μA

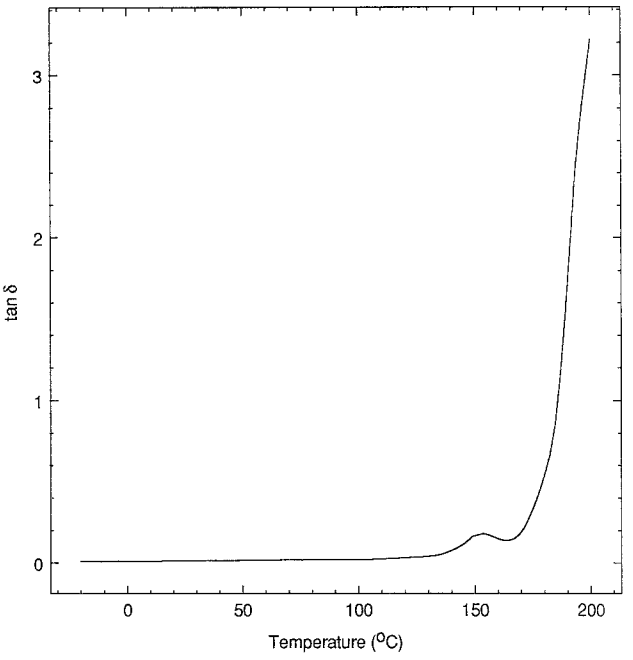

Fig. 9. The dielectric loss tan δ of P(MMA-CMA)-11 as a function of temperature measured at 0.1 Hz

in Fig. 8, did not significantly influence the $d_{\text{eff}}/d_{\text{quartz}}$ values measured at the increasing higher poling temperatures. The results indicate an increase by a factor of approximately 2.5 in second harmonic $d_{\text{eff}}/d_{\text{quartz}}$ for films poled at 160° C versus 100° C. The decreased second harmonic intensity for poling temperature of 175° C was most likely due to increased conductivity of the films or excessive thermal randomization of chromophore orientation. The measured dielectric loss of P(MMA-CMA)-11 is shown in Fig. 9. The conductivity increased significantly at temperatures above 165° C. The highest poling temperature (175° C) was still well below the measured onset of chemical decomposition (240° C) as was determined by thermogravimetric analysis at 2° C/min in nitrogen. The optimal poling temperature for a P(MMA-CMA) side-chain polymer was chosen to be 160° C at a poling current of 2 μA.

In P(MMA-CMA) side-chain polymer, the increased structural rigidity resulting from covalent attachment of the chromophore to the polymer necessitated poling temperatures of ≈ 30–40° C above T_g for optimal results. This is contrary to the behavior found in chromophore polymer mixtures, where poling was not as sensitive to temperature and current. Experiments with side-chain polymers having chromophores covalently attached to the backbone through three and five methylene spacer groups have shown poling behavior approaching that of mixtures. In the case of side-chain polymers with less than three methylene spacer groups, the chromophore and the polymer backbone are closely coupled and tend to move as one unit upon application of the poling field. Interaction between the chromophore and the polymer can be expected based on the length of the spacer group, size of the chromophore and the possibility of hydrogen bonding with the polymer. By heating the film to temperatures well above the T_g of the polymer, the motion of the dye chromophore and the polymer backbone become more decoupled through the disruptions of interactions, permitting more efficient alignment to be achieved through poling.

If dipole–dipole interactions are absent, a linear dependence of second-order polarizability on the chromophore density is predicted by the ROGM [7]. Side-chain polymers have a clear advantage over the mixtures (e.g. DR1/PMMA) since the concentration of nonlinear chromophore can be significantly higher. In the case of a mixture the solubility of the nonlinear molecules in the polymer host is limited. The stability and nonlinear molecular concentration can be increased by attaching the nonlinear constituents to a polymer backbone. For P(MMA-CMA) we have experimentally investigated the range in which negligible dipole–dipole interaction is present. P(MMA-CMA) substituted polymer films with dye concentrations of 2.2×10^{20}, 3.3×10^{20}, 5.7×10^{20}, and 9.8×10^{20} molecules/cm^3 were fabricated and corona poled under identical conditions. Figure 10 shows the second harmonic $d_{\text{eff}}/d_{\text{quartz}}$ dependence on the chromophore density. A linear extrapolation based on the available experimental data and error-bars indicate negligible dipole–dipole interaction in the range of chromophore densities that was investigated. This observation does seem to indicate that in nonlinear dye molecules with relatively small (compared to red shifted dyes) ground state dipole moment (μ = 5 D), dipole–dipole interactions effects become significant only at much larger chromophore concentrations. The lower hyperpolarizability can be compensated for by increased chromophore concentration, since the dipole–dipole interaction at a fixed concentration is smaller in the polymer with the lower dipole moment.

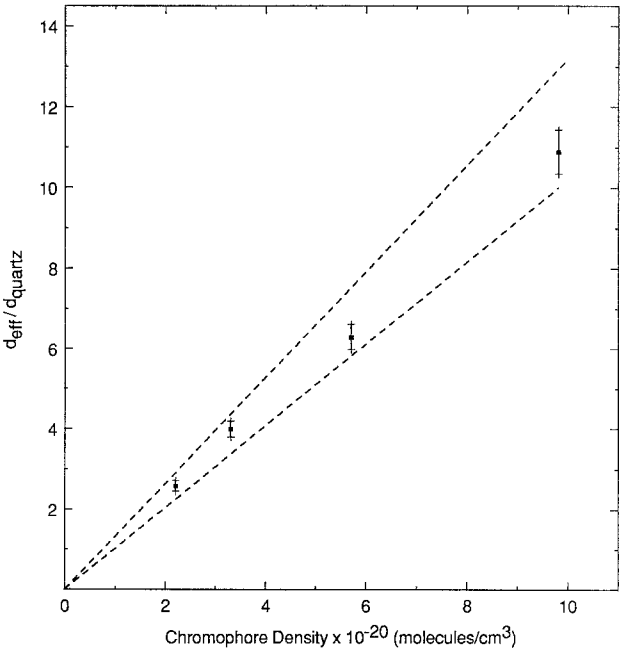

Fig. 10. Second harmonic $d_{\text{eff}}/d_{\text{quartz}}$ for COPET films of P(MMA-CMA) as a function of chromophore density

Second harmonic intensity measurements to quantify d_{33} were performed on a COPET P(MMA-CMA)-11 polymer film. The polymer film was $\approx 2.6\,\mu m$ thick, and was poled at the optimum poling condition: 160° C and $2\,\mu A$. Second harmonic measurements after poling indicated a small initial decay of less than 10% within the first 48 h, followed by a stabilization of nonlinear properties at room temperature, i.e. any fluctuations after 48 h were within the second harmonic measurement error. The initial decay can be contributed to decay of residual charges present on the film. The charge creates a residual electric field that enhances the nonlinear properties [7]. From the stabilized value of the second harmonic intensity, index of refraction and absorption measurements ($\Phi = 0.15$ and from Fig. 6, $\Lambda = 3.4$) it was concluded that $d_{33} = 13.0 \pm 1.3$ pm/V. This value for COPET P(MMA-CMA)-11, with a chromophore density of 9.8×10^{20} molecules/cm^3, correlates well with independently measured $d_{33} = 11$ pm/V [10] of a similar COPET P(MMA-CMA) copolymer, with a chromophore density of 9.0×10^{20} molecules/cm^3.

The long term stability of nonlinear properties in poled structures at temperatures exceeding room temperature is critical for practical applications. Devices are frequently exposed to high temperatures during fabrication, as a result of heat dissipation from surrounding electronic circuitry, and from the environment. The following experiment was performed to investigate the relaxation characteristics of P(MMA-CMA) copolymers at elevated temperatures. The temperature of a COPET P(MMA-CMA) film having stable nonlinear properties at room temperature was raised to 100° C and the second harmonic signal was monitored over a period of 40 h, see Fig. 11. Stabilization of the second harmonic intensity occurs at approximately 60% of the original signal after about 25 h. After 40 h, no further detectable decrease in second harmonic intensity was observed. Some decay can be expected since the poled films are not thermodynamically stable. However, this result does further indicate that the relaxation is not complete and substantial nonlinearity is retained.

2.2.2 Electro-Optic. A lack of understanding exists as to what determine the second-order nonlinear optical behavior in the vicinity of material resonances. We have performed an experimental investigation of the dispersion characteristics of the linear electro-optic coefficient, r_{33}. The experimental technique employed offers the flexibility to characterize nonlinear polymers in regions where absorption losses prohibit the utilization of guided wave electro-optic methods. The electro-optic coefficient, using the reflection technique, was calculated from [19, 23].

$$r_{33} = \frac{3\lambda I_m (n_f^2 - \sin^2\theta)^{1/2}}{4\pi V_m I_{1/2} n_f^2 \sin^2\theta}, \tag{6}$$

where I_m is the modulation amplitude of optical intensity, V_m is the applied modulating voltage, $I_{1/2}$ is the half intensity point, n_f is refractive index of the film, and θ is the incident angle outside the film. It is assumed that $r_{33} = 3r_{13}$ and poling induced birefringence is ignored; consistent with the contact electrode low poling field approximation. Figure 12 shows the dispersion characteristics of the electro-optic coefficient. The measured electro-optic coefficient was 1.9 pm/V at 1115 nm and as high as 11.9 pm/V at 477 nm. The extrapolated value of the electro-optic coefficient at 780 nm ($r_{33} = 2.5$ pm/V) for P(MMA-CMA)-11, with a chromophore density of

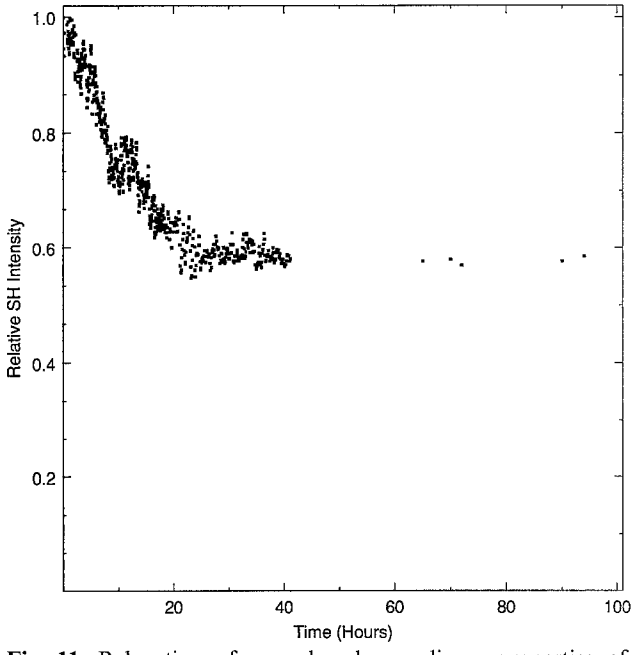

Fig. 11. Relaxation of second order nonlinear properties of a COPET P(MMA-CMA)-11 film held at 100° C, after aging at room temperature for several months

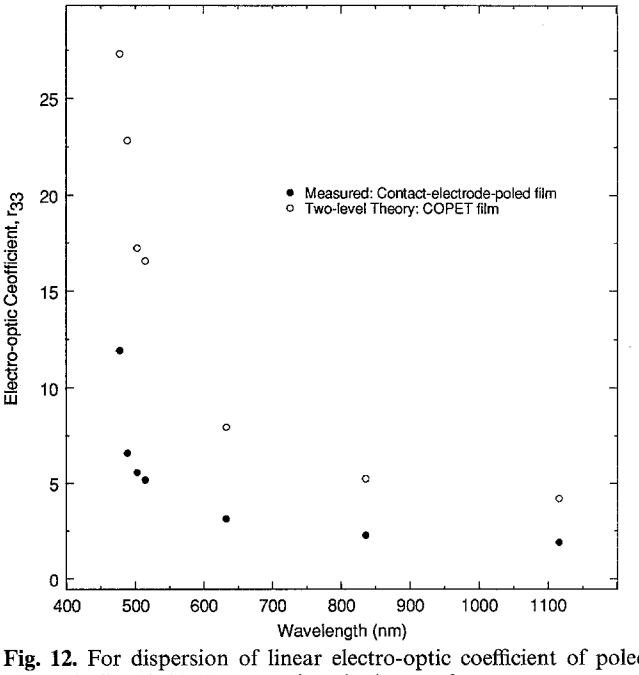

Fig. 12. For dispersion of linear electro-optic coefficient of poled P(MMA-CMA)-11. A comparison is shown of measurements were made on a contact-electrode-poled film with the two-level electro-optic theoretical predictions made from a second harmonic measurement on a corona-poled film

9.8×10^{20} molecules/cm^3, is smaller than reported in an independent guided wave measurement [10] of a similar P(MMA-CMA) copolymer, with a chromophore density of 9.0×10^{20} molecules/cm^3, $r_{33} = 3.5$ pm/V. This could be indicative of a lower orientational order. This observation is consistent with the different poling techniques used in the two studies. Contact-electrode-poled films were used in our electro-optic measurements, poled at a presumably lower poling field than the corona-poled films used in the guided wave measurements. As expected, a significant enhancement occured in the electro-optic coefficient for wavelengths that lie close to the main absorption band. This substantial enhancement of the electro-optic properties near resonance could be utilized in electro-optic device applications with short optical path length such as polymeric interference modulators [24].

A comparison of the measured electro-optic coefficient with a two-level dispersion theoretical model [25] was made. Electronic resonant contributions play a dominant role in polymers, and a two-level model predicts, from second harmonic measurements, the electro-optic coefficient dispersion behavior

$$r_{33} = \frac{4d_{33}f_\omega^2 f_0}{n^4(\omega) f_{2\omega'} f_{\omega'}^2} \frac{(3\omega_0^2 - \omega^2)(\omega_0^2 - \omega'^2)(\omega_0^2 - 4\omega'^2)}{3\omega_0^2(\omega_0^2 - \omega^2)^2}, \quad (7)$$

where ω is the operating frequency, ω' is the fundamental frequency used in the second harmonic measurements, $2\omega'$ is the second harmonic frequency used in the second harmonic measurements, ω_0 is the frequency of the first excited state, and f is the local field factor of Onsager type [26]. Figure 12 shows a comparison of the linear electro-optic dispersion as measured and predicted by the two-level molecular hyperpolarizability dispersion model. The measured values were made on a contact-electrode-poled film. The theoretical two level prediction was based on a SHG measurement on a COPET film. The absolute magnitude of the measured and calculated r_{33} coefficients were different due to the COPET film having a larger orientational order than the contact-electrode-poled film. The model gave a reasonable prediction of dispersion behavior far from resonance, but over corrects as the frequency of the electro-optic measurement approached resonance.

3 Conclusion

Films of P(MMA-CMA) were poled by both corona-onset and contact electrode techniques. The optimal corona poling temperature was approximately 40° C above the T_g of the polymer. Elevated temperature relaxation studies of poled P(MMA-CMA)-11 at 100° C revealed an initial decay in the second harmonic signal which stabilized at approximately 60% of the room temperature levels. We have reported the linear and nonlinear optical properties of a coumaromethacrylate side-chain nonlinear polymer. The refractive index (determined using prism coupling) and degree of orientational (determined by UV-Visible spectroscopy) were used in the extraction of second order nonlinear properties. The stabilized value of the second harmonic coefficient of the corona poled P(MMA-CMA)-11 film is ≈ 13 pm/V. The strong dispersion of the electro-optic coefficient of a poled film was measured and compared to theory.

Acknowledgements. This research was funded in part by IBM Corporation (MAM), National Science Foundation Grant ECS-9196012 (AK and STK), and Office of Naval Research (Naval Weapons Center, China Lake). We would like to thank M. C. Jurich and J. D. Swalen, IBM Research Division, Almaden Research Center, for the assistance in index measurements.

References

1. D.J. Williams (ed.): Nonlinear Optical Properties of Organic and Polymeric Materials, ACS Symp. Ser. 233 (1983)
2. D.S. Chemla, J. Zyss: (eds.): Nonlinear Properties of Organic Molecules and Crystals (Academic, New York 1987)
3. P.N. Prasad, D.R. Ulrich (eds.): Nonlinear Optical and Electroactive Polymers (Plenum, New York 1988)
4. A.J. Heeger, J. Orenstein, D.R. Ulrich (eds.): Nonlinear Optical Properties of Polymers, Mater. Res. Soc. Symp. Proc. **109** (1988)
5. R.A. Hann, D. Bloor: Organic Materials for Nonlinear Optics. Roy. Soc. Chem. Proc. **69** (1988)
6. A. Knoesen, M.A. Mortazavi, S.T. Kowel, A. Dienes, B.G. Higgins: In Nonlinear Optical Properties of Materials (Optical Soc. of Amer., Washington D.C. 1988) p. 244
7. M.A. Mortazavi, A. Knoesen, S.T. Kowel, B.G. Higgins, A. Dienes: J. Opt. Soc. Am. B **6**, 733–741 (1989)
8. D.J. Williams: Angew. Chem. Int. Ed. Engl. **23**, 690–703 (1984)
9. I. Ledoux, J. Zyss, A. Jutand, C. Amatore: Chem. Phys. **150**, 117–123 (1991)
10. L.M. Hayden, G.F. Sauter, F.R. Ore, P.L. Pasillas, J.M. Hoover, G.A. Lindsay, R.A. Henry: J. Appl. Phys. **68**, 456 (1990)
11. D.R. Yankelevich, A. Dienes, A. Knoesen, R.W. Schoenlein, C.V. Shank, G.A. Lindsay: Proc. of CLEO, Baltimore (1991) p. 602
12. R.A. Henry, J.M. Hoover, A. Knoesen, S.T. Kowel, G.A. Lindsay, M.A. Mortazavi: Mat. Res. Soc. Symp. Proc. **173**, 601–606 (1990)
13. R.A. Henry, J.M. Hoover, G.A. Lindsay: Navy Case NO. 72263 Patent disclosure (Oct. 1989)
14. A.C. Ouano: *Polymers in Electronics*, ed. by T. Davidson, ACS Symp. Ser. Washington D.C. (1984) p. 79
15. C.W. Lantman, J.F. Tassin, P. Sergot, L. Monnerie: Macromolecules **22**, 483 (1989)
16. J.D. Swalen, R. Santo, M. Tacke, J. Fischer: IBM J. Res. Develop. **3**, 168–175 (1977)
17. Stanford Research Systems, Fast Gated Integrators and Boxcar Averagers Operation Manual
18. D. Hass, H. Yoon, H.T. Man, G. Cross, S. Mann, N. Parsons: Proc. SPIE **1147**, 222 (1989)
19. C.C. Teng, H.T. Man: Appl. Phys. Lett. **56**, 1734–1736 (1990)
20. J. Jerphagon, S.K. Kurtz: J. Appl. Phys. **41**, 1667–1681 (1970)
21. R.H. Page, M.C. Jurich, B. Reck, A. Sen, R.J. Twieg, J.D. Swalen, G.C. Bjorklund, C.G. Wilson: J. Opt. Soc. Am. B **7**, 1239 (1990)
22. M. Eich, A. Sen, H. Looser, G.C. Bjorkland, J.D. Swalen, R. Twieg, D.Y. Yoon: J. Appl. Phys. **66**, 2559–2587 (1989)
23. An error in equation (10) of [19] is corrected, as per private communication with C.C. Teng
24. C.A. Eldering, A. Knoesen, S.T. Kowel: Proc. SPIE **1337**, 348–356 (1990)
25. K.D. Singer, S.L. Lalama, J.E. Sohn, R.D. Small: In *Nonlinear Optical Properties of Organic Molecules and Crystals*, D.S. Chemla, J. Zyss (eds.), Vol. 1 (Academic, New York 1987) pp. 437–468
26. L. Onsager: J. Chem. Soc. **58**, 1486–1493 (1936)